Published in final edited form as:
Angew Chem Int Ed Engl. 2011 March 1; 50(10): 2317–2321. doi:10.1002/anie.201007494.

Multifunctional Capsule-in-Capsules for Immunoprotection and Trimodal Imaging**

Dr. Jaeyun Kim,
Russell H. Morgan Department of Radiology and Radiological Science, Division of MR Research, Institute for Cell Engineering, Cellular Imaging Section, The Johns Hopkins University School of Medicine, Baltimore, MD 21205 (USA). National Creative Research Initiative Center for Oxide Nanocrystalline Materials, World Class University program of Chemical, Convergence for Energy and Environment, School of Chemical and Biological Engineering, Seoul National University, Seoul 151-744 (South Korea)

Dr. Dian R. Arifin,
Russell H. Morgan Department of Radiology and Radiological Science, Division of MR Research, Institute for Cell Engineering, Cellular Imaging Section, The Johns Hopkins University School of Medicine, Baltimore, MD 21205 (USA)

Dr. Naser Muja,
Russell H. Morgan Department of Radiology and Radiological Science, Division of MR Research, Institute for Cell Engineering, Cellular Imaging Section, The Johns Hopkins University School of Medicine, Baltimore, MD 21205 (USA)

Taeho Kim,
Russell H. Morgan Department of Radiology and Radiological Science, Division of MR Research, Institute for Cell Engineering, Cellular Imaging Section, The Johns Hopkins University School of Medicine, Baltimore, MD 21205 (USA). National Creative Research Initiative Center for Oxide Nanocrystalline Materials, World Class University program of Chemical, Convergence for Energy and Environment, School of Chemical and Biological Engineering, Seoul National University, Seoul 151-744 (South Korea)

Dr. Assaf A. Gilad,
Russell H. Morgan Department of Radiology and Radiological Science, Division of MR Research, Institute for Cell Engineering, Cellular Imaging Section, The Johns Hopkins University School of Medicine, Baltimore, MD 21205 (USA)

Dr. Heechul Kim,
Russell H. Morgan Department of Radiology and Radiological Science, Division of MR Research, Institute for Cell Engineering, Cellular Imaging Section, The Johns Hopkins University School of Medicine, Baltimore, MD 21205 (USA)

Dr. Aravind Arepally,
Russell H. Morgan Department of Radiology and Radiological Science, Division of MR Research, Institute for Cell Engineering, Cellular Imaging Section, The Johns Hopkins University School of Medicine, Baltimore, MD 21205 (USA)

**This work was supported by NIH RO1 EB007825 (J.W.M.B.), U54 CA151838 (J.W.M.B.), and the Maryland TEDCO Nanotechnology Fund (J.W.M.B.), and National Creative Research Initiative grant R16-2002-003-01001-0 (T.H.), Strategic Research grant 2010-0029138 (T.H.), and World Class University Program R31-10013 (T.H.) of the National Research Foundation (NRF) of Korea. Human islets were provided by the National Islet Cell Resource Center. J.W.M.B is a paid consultant for Surgivision, Inc. This arrangement has been approved by The Johns Hopkins University in accordance with its Conflict of Interest policies.

*Fax: (+1)443-287-7945, jwmbulte@mri.jhu.edu, Fax: (+82)2-886-8457, thyeon@snu.ac.kr.

Supporting information for this article is available on the WWW under http://dx.doi.org/10.1002/anie.201007494.

Prof. Taeghwan Hyeon[*], and
National Creative Research Initiative Center for Oxide Nanocrystalline Materials, World Class University program of Chemical, Convergence for Energy and Environment, School of Chemical and Biological Engineering, Seoul National University, Seoul 151-744 (South Korea)

Prof. Jeff W. M. Bulte[*]
Russell H. Morgan Department of Radiology and Radiological Science, Division of MR Research, Institute for Cell Engineering, Cellular Imaging Section, The Johns Hopkins University School of Medicine, Baltimore, MD 21205 (USA)

Keywords

capsules; cell delivery; imaging agents; insulin; nanostructures

Type I diabetes mellitus (T1DM) is a T-cell-mediated autoimmune disease that results in destruction of insulin-producing β cells and subsequent hyperglycemia.[1,2] The current way of treating T1DM is insulin replacement therapy through repetitive injections of recombinant insulin. In more serious cases, a cadaveric pancreas[3] or purified pancreatic islets[4,5] can be transplanted to restore proper glucose regulation. However, the risks of surgery and the accompanying life-long immunosuppression outweigh the disadvantages of continued administration of insulin. The immunoisolation of islets by alginate microencapsulation is an emerging and promising solution to circumvent immune rejection and so overcome this limitation.[6] While the semipermeable alginate membrane blocks penetration of immune cells and antibodies, it allows the unhindered passage of nutrients, metabolites, and insulin that are produced by encapsulated islet cells.[7] Intraperitoneal administration of microencapsulated islets in monkeys and humans has showed considerable promise for the treatment of T1DM.[8,9]

Despite the therapeutic successes of cell therapy for T1DM, it has been difficult to assess the accuracy of transplantation and the extent of the engraftment of naked and microencapsulated cells. If transplanted microcapsules could be detected by clinically applicable non-invasive imaging modalities, including magnetic resonance (MR), computed tomography (CT), and ultrasound (US) imaging, the efficacy of transplantation and engraftment could be monitored repeatedly over time. Recently, a variety of nanoparticles, including magnetic nanoparticles, quantum dots, and gold nanoparticles, have been used as contrast agents for the non-invasive imaging of tumors, transplanted islets, macrophages, and other tissues.[10–20] We have previously shown that co-encapsulation of islet cells in alginate capsules with iron oxide nanoparticles,[21] barium sulfate,[22] or perfluorocarbons[23] allows non-invasive tracking with MR, X-ray, or multimodal imaging, respectively. In general, a high payload of nanoparticles is required to achieve a sufficient amount of contrast. However, nanoparticles used for imaging purposes can potentially be toxic to the cells at higher concentrations.[24,25] We hypothesized that by encapsulating nanoparticles in a primary inner capsule within the secondary outer capsule, in which the therapeutic islet cells reside, nanoparticle-associated toxicity could potentially be mitigated. We report here on the synthesis of such “capsule-in-capsules” (CICs) containing gold, iron oxide, and islet cells (Figure 1a), and demonstrate that these CICs can be tracked with three modalities (MR, CT, and US imaging) while maintaining cell viability and glucose responsiveness both in vitro and in vivo, as demonstrated by their ability to restore normal glycemia levels in streptozotocin-induced diabetic mice.

We considered two important factors for the successful fabrication of CICs. First, the alginate concentration of the inner secondary core alginate capsule should be higher than that of the primary outer alginate capsule. We observed that, because of differences in

osmotic pressure, the primary capsule shrinks during synthesis in the presence of a secondary alginate solution of a higher concentration (see Figure S1 in the Supporting Information), which causes the nanoparticles to eventually be released into the secondary outer alginate capsule. In contrast, the spherical morphology of the core capsules was maintained when the primary capsules were synthesized with a higher alginate concentration.

Second, instead of Ca^{2+} ions, the most commonly used divalent cationic cross-linker for the gluronic acid (G) block of the alginate polymer, we used Ba^{2+} ions as a stronger cross-linker.[26] The cross-linking stability of the dual capsule system is of key importance in maintaining overall integrity of the CICs. When Ca^{2+} ions were used in the synthesis of CICs, both the primary and secondary capsules swelled readily and resulted in a 1.5–2-fold increase in the capsule diameter compared to the initial size (see Figures S1 and S2 in the Supporting Information). In contrast, the size of both capsules remained unchanged when Ba^{2+} ions were used (see Figure S2 in the Supporting Information). Figure 1b shows a successful fabrication of CICs, in which a high initial alginate concentration was used for the primary capsules and Ba^{2+} ions used as a cross-linker. Primary alginate capsules containing Feridex (dextran-coated iron oxide nanoparticles) and gold nanoparticles[27,28] were prepared by using 2.0% w/v alginate and Ba^{2+} ions. The loading of nanoparticles can be easily controlled by varying the amount of nanoparticles in the alginate solution (see Figure S3 in the Supporting Information). The resulting primary capsules were encapsulated again with 1.8% w/v alginate and cross-linked with Ba^{2+} ions to produce CICs with a double capsule structure. The resulting CICs did not show any increase in their overall size and there was no release of the nanoparticles from the primary to the secondary capsules for at least 3 months. Mouse insulinoma cells were successfully encapsulated in the secondary alginate capsule of the CIC (Figure 1c), with 90% viability post-encapsulation (Figure 1d).

Next, to test our hypothesis that cell function is not hindered by nanoparticles as a result from the physical barrier within CICs, we fabricated three different types of alginate capsules encapsulated with human islets (Figure 2a): islets encapsulated within a single capsule without nanoparticles (unlabeled CAPs; Figure 2b); islets co-encapsulated with gold and iron oxide within a single capsule (NP-CAPs; Figure 2c); and labeled CICs (Figure 2d). Islets could not be visualized in the case of NP-CAPs because of the high density of gold and iron oxide nanoparticles. The size of these three capsule types was similar (around 800 μm in diameter). To determine the viability of human islets for each of the three preparations, islets were stained with fluorescein diacetate (FDA), (Figure 2b–d bottom images), a marker for live cells, as the dye is rapidly hydrolyzed to fluorescein only when intracellular active esterase is present. The relative viability of cells in the NP-CAPs and labeled CICs compared with FDA-staining in unlabeled CAPs were 13% and 97%, respectively.

In addition to fluorescent viability staining for an assessment of whether the physical separation between nanoparticles and cells within CICs leads to a better overall preservation of cell function, we tested the insulin secretion by human islets for each type of capsule. For measuring glucose responsiveness at one day post-encapsulation, capsules were first incubated in glucose-free media for 1.5 h. The capsules were then incubated with 3.3 mM glucose followed by 16.7 mM glucose for 45 minutes each. Aliquots of culture medium were collected and assayed for human c-peptide (insulin) secretion by using a human c-peptide enzyme-linked immunosorbent assay (ELISA). Insulin secretion at 3.3 mM was comparable for all three capsule types (Figure 2e). However, at 16.7 mM glucose, the insulin secretion of NP-CAPs was significantly lower (7.77 ± 1.14 pg c-peptide per islet) than that of unlabeled CAPs (20.0 ± 0.66 pg c-peptide per islet) and CICs (16.0 ± 1.12 pg c-peptide per islet; Figure 2e, $P = 0.001$). The glucose responsiveness stimulation index, as

defined by the increase in insulin secretion after changing from 3.3 to 16.7 mM glucose solution, was 5.0 ± 0.62, 2.6 ± 0.31, and 3.4 ± 0.41 for unlabeled CAPs, NP-CAPs, and CICs, respectively. To assess the changes in insulin production over time, c-peptide secretion was assessed at high glucose media (24.9 mM) for a period of 23 days (Figure 2f). In agreement with the glucose responsiveness results, prolonged insulin secretion from human islets in CICs was comparable to that from unlabeled CAPs and significantly higher than that from NP-CAPs starting at day 3 ($P = 0.004$). Taken together, these data suggest that when nanoparticles are separated from the islets by a physical barrier present in the CICs there is improved preservation of cell function compared to NP-CAPs, where nanoparticles of gold and iron oxide are in direct contact with islet cells.

Next, the CICs were tested for visualization by MRI, CT, and US imaging. Phantoms were prepared in 2 w/v% agarose for MRI and micro-CT, and in 10 mM phosphate buffered saline (PBS) for US imaging. The concentrations of Fe and Au per CIC, as measured by inductively coupled plasma atomic emission spectroscopy (ICP-AES), were 0.156 μg per CIC and 1.38 μg per CIC, respectively. Feridex-containing CICs induced a substantial reduction of the signal in T_2-weighted MR images and could be clearly identified at the single capsule level as single hypointensities (Figure 3a). The higher absorption coefficient (5.16 cm^2g^{-1} and 1.94 cm^2g^{-1} of gold and iodine at 100 kV, respectively) and a smaller molecular weight results in gold providing a contrast that is about 2.7 times greater per unit weight than iodine, a standard contrast agent in CT imaging.[18] As a result, CICs showed strong signal attenuation with micro-CT (Figure 3b). Single CICs with a unique double capsule structure were also clearly visible by US imaging (Figure 3c).

Subsequently, 500 and 1200 CICs or saline as control were transplanted into the peritoneal cavity of female C57BL/6 mice—this anatomical site has been widely used as the transplantation site for encapsulated islet cell therapy.[7,8,21,22] Both spin-echo and gradient-echo MRI revealed the CICs as single hypointensities (Figure 3d,e) that corresponded with the number of CICs transplanted. A similar pattern of radiopacity was observed by micro-CT (Figure 3f). The anatomical location of the CICs, again with a distinct double capsule structure, could also be clearly determined by US imaging (Figure 3g, and see the movie in the Supporting Information). The contrast of the CICs was persistent for at least 3 months by MRI, micro-CT, and US imaging, thus demonstrating the excellent stabilization of the nanoparticles within the double capsule structure.

Finally, to evaluate the therapeutic potential of cells encapsulated in the CICs, CICs containing beta-TC-6 mouse insulinoma cells[21,29] were transplanted into the peritoneum of streptozotocin-induced diabetic mice. Streptozotocin destroys the native insulin-producing beta cells of the pancreas through the glucose transport protein GLUT2 that is highly expressed by pancreatic beta cells.[30] Diabetic mice were divided into two groups (n =6 each): one injected with CICs containing beta-TC-6 cells, and a control group injected with saline. The peritoneal cavity contains sufficient space to accommodate the total capsular volume and enables rapid access of the insulin to the liver, the major organ for insulin consumption.

Blood glucose levels and animal body weights were recorded over 8 weeks at 2–4 day intervals. For the CIC group, blood glucose levels returned to normal levels (<200 $mgdl^{-1}$) immediately after transplantation and was maintained for at least 75 days (Figure 4a). This was not the case for the control group, where glucose levels remained at >500 $mgdl^{-1}$. The CIC mice initially exhibited a 10% weight loss, but their weights exceeded those of the control groups after 3 weeks post-transplantation and continued to be higher throughout the entire course of the experiment (Figure 4b). The total net average weight increase during the

observation period was 1.8-fold higher for CIC mice (7.4 g, compared to 4.2 g for control mice; Figure 4b).

The CICs were visualized in vivo by MRI, micro-CT, and ultrasound imaging 3 months post-transplantation. To this end, diabetic mice were injected intraperitoneal (i.p.) with 500 CICs containing 3×10^6 mouse insulinoma cells. Single CICs could be clearly detected with every imaging modality; the imaging images at 3 months were similar to those immediately after the transplantation (see Figure S4 in the Supporting Information). Four months after transplantation, CICs were recovered from the abdomen and stained with fluorescein diacetate (FDA) and propidium iodide (PI) to determine cell viability (Figure 4c). Cell viability was found to be 55%, and the recovered CICs were further tested for insulin secretion. The recovered CICs had an intact appearance without breakage, which suggests that Ba^{2+} ions can indeed be used as a strong, efficient cross-linker. There was no apparent nanoparticle-associated toxicity in vivo, thus indicating that the double capsule structure prevents the leakage of particles from the CICs. Thirty CICs were recovered from each treatment group and the secreted amount of c-peptide in culture medium was measured daily for 3 days (Figure 4d). Cells continued to produce significant levels of c-peptide in vitro, in agreement with the observed prolonged normoglycemia in vivo.

In conclusion, we have developed novel capsule-in-capsules for immunoprotection and trimodal imaging by MRI, CT, and US. This possibility opens the door to the non-invasive determination of the spatial and temporal kinetics of the quantity and location of transplanted islets. By separating the islets not only from the immune system but also from nanoparticles we have demonstrated an excellent preservation of islet glucose responsiveness both in vitro and in vivo. We anticipate that this may lead to further optimization of cell therapy in a microprotected environment.

Supplementary Material

Refer to Web version on PubMed Central for supplementary material.

References

1. Liblau RS, Wong FS, Mars LT, Santamaria P. Immunity. 2002; 17:1. [PubMed: 12150886]
2. Savinov AY, Burn P. Drug Discovery Today. 2010; 15:531. [PubMed: 20685342]
3. Larsen JL. Endocr Rev. 2004; 25:919. [PubMed: 15583023]
4. Shapiro AM, Lakey JR, Ryan EA, Korbutt GS, Toth E, Warnock GL, Kneteman NM, Rajotte RV. N Engl J Med. 2000; 343:230. [PubMed: 10911004]
5. See the Supporting Information for the full reference.
6. Lim F, Sun AM. Science. 1980; 210:908. [PubMed: 6776628]
7. Zimmermann H, Shirley SG, Zimmermann U. Curr Diabetes Rep. 2007; 7:314.
8. Soon-Shiong P, Heintz RE, Merideth N, Yao QX, Yao Z, Zheng T, Murphy M, Moloney MK, Schmehl M, Harris M, et al. Lancet. 1994; 343:950. [PubMed: 7909011]
9. Zhou D, Sun YL, Vacek I, Ma P, Sun AM. Transplant Proc. 1994; 26:1091. [PubMed: 8029840]
10. Bulte JW, Kraitchman DL. NMR Biomed. 2004; 17:484. [PubMed: 15526347]
11. Na HB, Song IC, Hyeon T. Adv Mater. 2009; 21:2133.
12. Lee JH, Huh YM, Jun YW, Seo JW, Jang JT, Song HT, Kim S, Cho EJ, Yoon HG, Suh JS, Cheon J. Nat Med. 2007; 13:95. [PubMed: 17187073]
13. Gao X, Cui Y, Levenson RM, Chung LW, Nie S. Nat Biotechnol. 2004; 22:969. [PubMed: 15258594]
14. Medintz IL, Uyeda HT, Goldman ER, Mattoussi H. Nat Mater. 2005; 4:435. [PubMed: 15928695]
15. Choi HS, Liu W, Liu F, Nasr K, Misra P, Bawendi MG, Frangioni JV. Nat Nanotechnol. 2010; 5:42. [PubMed: 19893516]

16. Kim J, Piao Y, Hyeon T. Chem Soc Rev. 2009; 38:372. [PubMed: 19169455]
17. Gao J, Gu H, Xu B. Acc Chem Res. 2009; 42:1097. [PubMed: 19476332]
18. Hainfeld JF, Slatkin DN, Focella TM, Smilowitz HM. Br J Radiol. 2006; 79:248. [PubMed: 16498039]
19. Evgenov NV, Medarova Z, Dai G, Bonner-Weir S, Moore A. Nat Med. 2006; 12:144. [PubMed: 16380717]
20. Hyafil F, Cornily JC, Feig JE, Gordon R, Vucic E, Amirbekian V, Fisher EA, Fuster V, Feldman LJ, Fayad ZA. Nat Med. 2007; 13:636. [PubMed: 17417649]
21. Barnett BP, Arepally A, Karmarkar PV, Qian D, Gilson WD, Walczak P, Howland V, Lawler L, Lauzon C, Stuber M, Kraitchman DL, Bulte JW. Nat Med. 2007; 13:986. [PubMed: 17660829]
22. Barnett BP, Kraitchman DL, Lauzon C, Magee CA, Walczak P, Gilson WD, Arepally A, Bulte JW. Mol Pharm. 2006; 3:531. [PubMed: 17009852]
23. Barnett BP, Ruiz-Cabello J, Hota P, Liddell R, Walczak P, Howland V, Chacko VP, Kraitchman DL, Arepally A, Bulte JW. Radiology. 2011; 258:182. [PubMed: 20971778]
24. Hussain SM, Braydich-Stolle LK, Schrand AM, Murdock RC, Yu KO, Mattie DM, Schlager JJ, Terrones M. Adv Mater. 2009; 21:1549.
25. Lewinski N, Colvin V, Drezek R. Small. 2008; 4:26. [PubMed: 18165959]
26. Mørch YA, Donati I, Strand BL, Skjåk-Braek G. Biomacromolecules. 2006; 7:1471. [PubMed: 16677028]
27. Enustun BV, Turkevich J. J Am Chem Soc. 1963; 85:3317.
28. Wang H, Halas NJ. Adv Mater. 2008; 20:820.
29. Sakai S, Ono T, Ijima H, Kawakami K. J Sol-Gel Sci Technol. 2003; 28:267.
30. Wang Z, Gleichmann H. Diabetes. 1998; 47:50. [PubMed: 9421374]

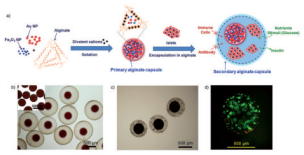

Figure 1.
CICs enable physical separation of cells and nanoparticles. a) Schematic representation of the composition of the CICs: the primary capsule contains iron oxide and gold nanoparticles, while the secondary-capsule contains islet cells. b) Microscopy image of the CICs (inset: primary microcapsules containing iron oxide and gold nanoparticles). c) Microscopy image of CICs containing beta-TC-6 mouse insulinoma cells present within the shell capsule. d) Viability staining (green =FDA, live cells; red =PI, dead cells) of mouse insulinoma encapsulated in CICs at 48 h after encapsulation demonstrates approximately 90% cell viability.

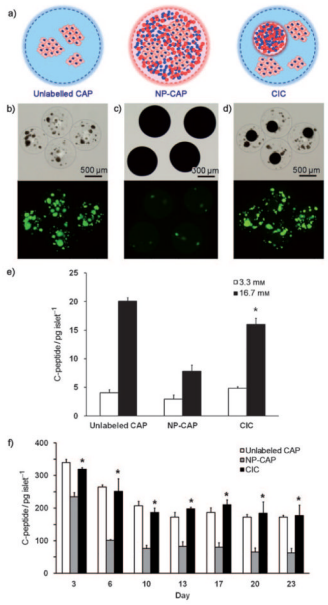

Figure 2.

In vitro function of human islets in CICs is superior compared to that of NP-CAPs. a) Schematic representation of the encapsulation of human islets in unlabeled CAPs, NP-CAPs, and CICs. b)–d) Microscopy images (upper rows) and corresponding live-cell staining with FDA (bottom rows). e) Glucose responsiveness of encapsulated human islets at 37°C for 3.3 mM (open bars) and 16.7 mM (solid bars) glucose in Dulbecco's modified Eagle's medium (DMEM) media supplemented with 15 % fetal bovine serum (FBS). f) Time-dependent insulin secretion of encapsulated human islets for unlabeled CAPs (open bars), NP-CAPs (gray solid bars), and CICs (black solid bars) at 37°C in DMEM media supplemented with 15% FBS. Asterisks indicate a statistically significant difference in the secretion between NP-CAPs and CICs (P <0.05).

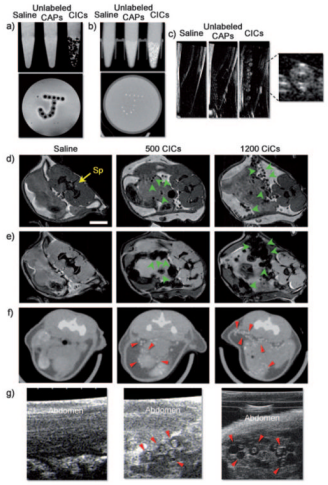

Figure 3.

In vitro and in vivo multimodal imaging with CICs. a) Spin-echo 9.4 T MRI, b) micro-CT, and c) US imaging of phantoms containing saline, unlabeled CAPs, and CICs. d) Spin-echo MRI, e) gradient-echo MRI, f) micro-CT, and g) US imaging 1 day after injection of the mouse abdomen with saline, 500, or 1200 CICs. Sp =spinal cord. Note that single CICs can be clearly identified (arrows) in vitro and in vivo.

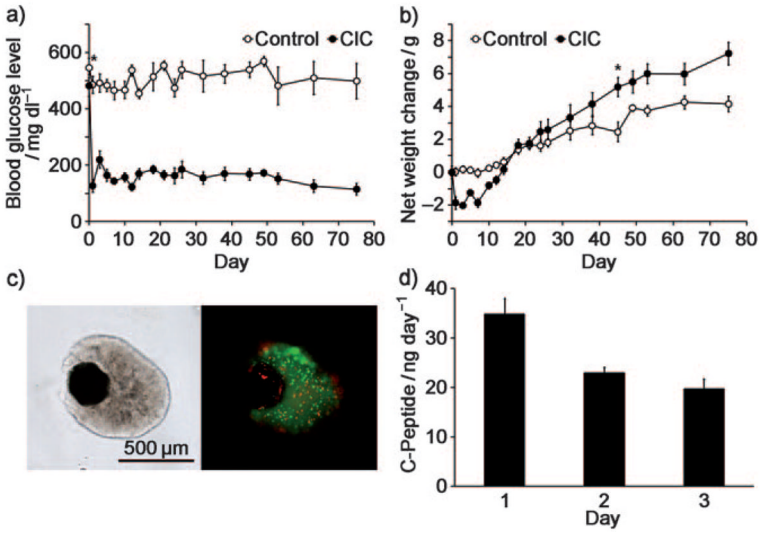

Figure 4.

Mouse insulinoma cells encapsulated in CICs restore normal glucose levels in diabetic mice. a) Blood glucose levels and b) weight changes in streptozotocin-induced diabetic mice after intraperitoneal transplantation of 500 CICs (3×10^6 insulinoma cells; closed symbols, n =6) or without transplantation of CICs (open symbols, n =6). Asterisks in (a, b) indicate the day on which the difference in the values between the two groups became significant (P<0.05). c) FDA and PI viability stainings of CICs containing mouse insulinoma cells recovered from a diabetic mouse 4 months after transplantation shows >50 % cell viability. d) C-peptide secretion (3 day accumulation) of 30 CICs recovered from a diabetic mouse 4 months after transplantation.